An agent-based model to simulate SARS-CoV-2 contamination of surfaces and meat cuts in processing plants

Ngoc-Du Martin Luong, Laurent Guillier, Michel Federighi, Yvonnick Guillois, Pauline Kooh, Anne-Laure Maillard, Mathilde Pivette, Géraldine Boué, Sandra Martin-Latil, Estelle Chaix, et al.

An agent-based model to simulate SARS-CoV-2 contamination of surfaces and meat cuts in processing plants

Ngoc-Du Martin Luong, Laurent Guillier, Michel Federighi, Yvonnick Guillois, Pauline Kooh, Anne-Laure Maillard, Mathilde Pivette, Géraldine Boue, Sandra Martin-Latil, Estelle Chaix, Steven Duret

PII: S0168-1605(23)00237-4

DOI: https://doi.org/10.1016/j.ijfoodmicro.2023.110321

Reference: FOOD 110321

To appear in: *International Journal of Food Microbiology*

Received date: 3 March 2023

Revised date: 24 May 2023

Accepted date: 10 July 2023

Please cite this article as: N.-D.M. Luong, L. Guillier, M. Federighi, et al., An agent-based model to simulate SARS-CoV-2 contamination of surfaces and meat cuts in processing plants, *International Journal of Food Microbiology* (2023), https://doi.org/10.1016/j.ijfoodmicro.2023.110321

Revised manuscript

Title

An agent-based model to simulate SARS-CoV-2 contamination of surfaces and meat cuts in processing plants

Journal

International Journal of Food Microbiology – Special Issue "VSI: Next Generation Challenges"

Authors

Ngoc-Du Martin LUONG[1*] (ngoc-du.luong@anses.fr, ORCID: 0000-0003-0714-136X)

Laurent GUILLIER[1*] (laurent.guillier@anses.fr, ORCID: 0000-0002-78[illegible]7-2937)

Michel FEDERIGHI[2,3,4] (michel.federighi@vet-alfort.fr, ORCID: 0000-0002-1108-6490)

Yvonnick GUILLOIS[5] (yvonnick.guillois@santepubliquefrance.fr, ORCID: 0000-0003-3069-3779)

Pauline KOOH[1] (pauline.kooh@anses.fr, ORCID: 0000-0002-7[illegible]06-9617)

Anne-Laure MAILLARD[5] (anne-laure.maillard@ehesp.fr)

Mathilde PIVETTE[5] (mathilde.pivette@santepubliquefrance.fr, ORCID: 0000-0002-1867-1561)

Géraldine BOUE[2] (geraldine.boue@oniris-nantes.fr, ORCID: 0000-0003-3716-8352)

Sandra MARTIN-LATIL[4] (sandra.martin-latil@anses.fr)

Estelle CHAIX[1] (estelle.chaix@anses.fr, ORCID: 0000-0003-0975-7854)

Steven DURET[6] (steven.duret@inrae.fr, ORCID: 0000-0002-9293-8092)

* These authors contributed equally as first authors to this work

Affiliation

[1] Risk Assessment Department, ANSES, Maisons-Alfort, France

[2] UMR INRAE 1014 SECALIM, Oniris, Nantes, Cedex 03, France

[3] ENVA, 94701 Maisons-Alfort, France

[4] Laboratory for Food Safety, ANSES, University of Paris-EST, Maisons-Alfort, France

[5] Regions Department, Santé Publique France (SpFrance), the French National Public Health Agency, Rennes, France

[6] Université Paris-Saclay, FRISE, INRAE, Antony, France

Corresponding author

Ngoc-Du Martin LUONG[1] (ngoc-du.luong @anses.fr)

Abstract

At the beginning of the COVID-19 pandemic, several contamination clusters were reported in food-processing plants in France and several countries worldwide. Therefore, a need arose to better understand viral transmission in such occupational environments from multiple perspectives: the protection of workers in hotspots of viral circulation; the prevention of supply disruption due to the closure of plants; and the prevention of cluster expansion due to exports of food products contaminated by the virus to other locations. This paper outlines a simulation-based approach (using agent-based models) to study the effects of measures taken to prevent the contamination of workers, surfaces, and food products. The model includes user-defined parameters to integrate characteristics relating to SARS-CoV-2 (variant of concern to be considered, symptom onset...), food-processing plants (dimensions, ventilation...), and other sociodemographic transmission factors based on laboratory experiments as well as industrial and epidemiological investigations. Simulations were performed for a typical meat-processing plant in different scenarios for illustration purposes. The results suggested that increasing the mask-wearing ratio led to great reductions in the probability of observing clusters of more than 25 infections. In the case of clusters, masks being worn by all workers limited the presence of contamination (defined as levels of at least 5 $\log_{10}$ viral RNA copies) on meat cuts at less than 0.05% and maintained the production capacity of the plant at optimal levels. Increasing the average distance between two workers from less than 1m to more than 2m decreased the cluster-occurrence probability by up to 15% as well as contamination of food products during cluster situations. The developed approach can open up several perspectives in terms of potential communication-support tools for the agri-food sector and further reuses or adaptations for other hazards and occupational environments.

Keywords

Coronavirus, viral transmission, occupational environment, preventive measure

Abbreviations

- ABM Agent-based model / Agent-based modeling

Colors should be used for all figures in print

1 Introduction

During the first months of the COVID-19 pandemic in 2020, several contamination clusters were observed in the occupational environments of essential sectors in different countries, such as healthcare centers (Airoldi et al., 2020; Magnusson et al., 2021), public establishments with social gatherings such as schools (Fontanet et al., 2021), and food-processing plants (Dyal et al., 2020; Mallet et al., 2021; Steinberg et al., 2020). In France, from the first lockdown period (March to May 2020), workers in the food-production sector were considered an essential workforce, since food-processing plants' activities had to remain uninterrupted in order to avoid any disruption occurring in the food-supply chain. In its national report of August 2020, the French National Public Health Agency reported 28 clusters in food-processing plants (20 of those being in meat-processing plants) out of the 189 clusters in occupational environments registered from May 9th to August 12th, 2020 (Santé Publique France, 2020). Preventing SARS-CoV-2 clusters in food-processing plants presents a great challenge, since viral transmission in these occupational environments is poorly understood. Indeed, workers in food-processing plants might be exposed to a high risk of infection mainly due to their close contact with each other in their working environment. However, infections caused by respiratory viruses like SARS-CoV-2 might be influenced by multiple factors. One can cite, for example, influences from variations in the plants' characteristics, such as their airflow, ventilation, temperature, etc. (Bazant and Bush, 2021; Chaudhuri et al., 2020; Kennedy et al., 2021); inter-individual differences in terms of infectiousness or symptom onset (Alene et al., 2021; He et al., 2021; Jones et al., 2021; Teyssou et al., 2021); and also the introduction of preventive and control measures like mask-wearing and physical distancing (Backer et al., 2021; Leech et al., 2022). In addition, clusters in food-processing plants could hypothetically spread to other, distant locations due to exports of food products possibly being contaminated by the virus. This hypothesis has been suggested to explain the reappearance of COVID-19 in cities with no observed cases for more than 90 days (Han et al., 2020). Thus, there was a need to carefully study viral transmission in food-processing plants from three perspectives: (i) to protect

workers and prevent these plants from becoming hotspots of viral transmission; (ii) to prevent closure of food plants and ensure supplies; and (iii) to prevent food contamination and avoid potential export of the virus to other locations.

This paper aimed to gain insights into the circulation of SARS-CoV-2 in food-processing plants by developing a simulation-based modeling approach capable of studying the effects of preventive measures carried out simultaneously against the contamination of workers, surfaces, and food products present in the plants. As surfaces and food portions can be contaminated due to the virus spreading between workers at the plant, an original agent-based model (ABM) was developed that included various possible routes of transmission (aerosol sedimentation of small droplets, direct contamination by larger droplet projections and transfer by contact from surface to surface while including different worker behaviors and operating conditions (mask-wearing ratio, distance between workers, air renewal, coughing, sneezing…). A simulation workflow with a detailed analysis of this contamination is illustrated in this paper, as well as the effect of two preventive measures. In numerical simulations, it is possible to include different characteristics relating to both SARS-CoV-2 and food-processing plants. Considering the clusters reported in the literature, we chose the application case of a meat-processing plant. For this paper, this simulation-based approach was used and is illustrated herein for the purpose of pointing out the potential effects of the implementation of two preventive measures regarding contamination inside a meat-processing plant, namely raising the mask-wearing ratio and increasing the physical distancing between workers.

2 Materials and methods

2.1 Overview of the model description

The modeling work presented in this paper was part of a collaborative multidisciplinary project (SACADA Project, Grant ANR-21-CO13-0001, funded by the French National Research Agency). The

outline of the ABMapproach developed is schematized in Figure 1. This model simulated the transmission of SARS-CoV-2 in a multi-room meat-processing plant and provided, as simulation outputs, several indicators describing possible infections of the workers as well as the food and/or contamination of surfaces. A short description is presented below to provide readers with an overview of the model. The mathematical formalization is not detailed herein since it goes beyond the scope of this paper (currently the subject of an ongoing article submission, a detailed description of which can be accessed at ndmluong.quarto.pub/sacada-project. The accessibility of this online model description is susceptible to change according to the peer-review-process status).

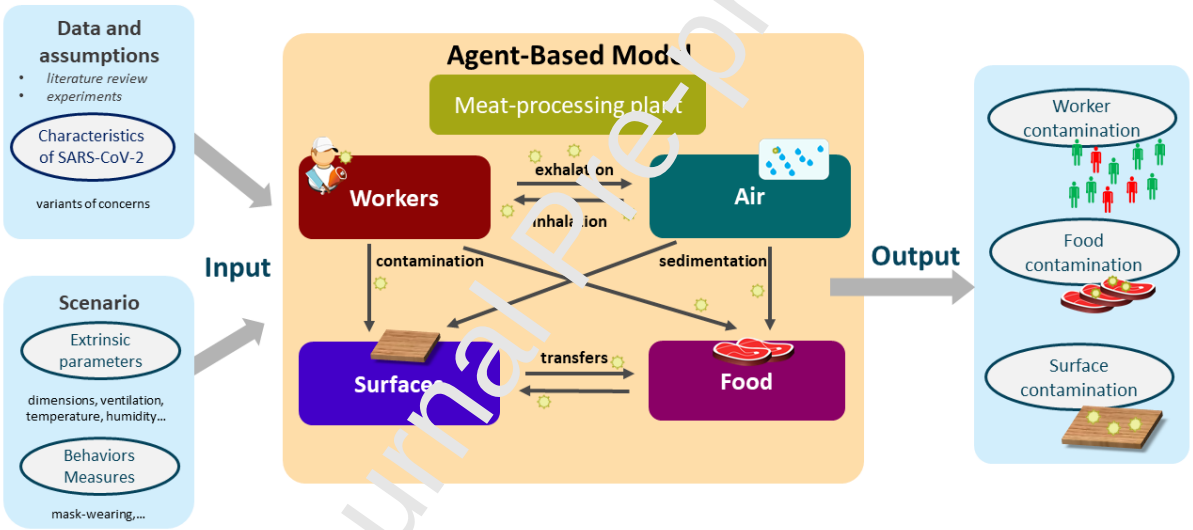

Figure 1 – Outline of the agent-based model to simulate the transmission of SARS-CoV-2 in multi-room meat-processing plants

The developed model was composed of several separate modules for describing the different agents present in the processing plants as well as possible interactions between them. These agents belonged to four main modules, corresponding, respectively, to (i) the workers, (ii) the droplets present in the air and/or on surfaces, (iii) the different small fractions of inert surfaces, and (iv) the food (meat) portions present in the plant. As shown in Figure 1, the model described the viral transmission through possible interactions between these agents. These interactions included, firstly, the transfer of droplets (containing or free from infectious viral particles) between the workers and the air through

respiratory activities such as exhalation and inhalation during the working day. Depending on the ventilation system, a portion of the droplets emitted by infectious workers can settle on different inert surfaces as well as on food portions present in the plant. These surfaces and food portions could also become contaminated due to direct projections of large droplets emitted due to SARS-CoV-2 symptoms such as frequent coughing and/or sneezing events. Finally, transfers of contaminated droplets were also possible due to contact between inert surfaces and food portions.

Several parameters were taken into account in the model (the parameter table is provided online in *Supplementary materials, Table S1*). On the one hand, there were parameters considered as input data and identified from the literature data/assumptions or preliminary laboratory experiments regarding the characteristics of SARS-CoV-2. One can cite, for example, the development of symptoms depending on the variant of the virus under consideration. On the other hand, based on industrial and epidemiological investigations, other parameters were included to simulate the behavior of the model in different scenarios. These scenarios were determined by defining extrinsic environmental parameters (such as the plant dimensions, ventilation, etc.). Worker behaviors, such as mask-wearing or physical distancing, were also specified and varied in the defined scenarios, which could be useful for evaluating the potential effects of control measures relating to viral transmission.

Based on prior data and knowledge, spatiotemporal rules were defined to simulate the interactions between modules and the properties of every agent at successive time points distanced by a predefined short time step. These step-by-step simulations were performed afterward for longer periods (days, weeks, etc.). At the end of these periods, balances were calculated for different properties of the agents, e.g. the total number of aerosolized or fallen droplets, the number of viral gene copies inhaled by each worker possibly triggering an infection. Based on these balances, several contamination indicators were estimated, such as the total number of infected workers over a several-day period and the daily number of contaminated food portions and surfaces in the plant. The results

of these estimated indicators were explored in this paper for comparison purposes between the studied scenarios.

2.2 Scenario analysis

The sections below describe the main parameters necessary for analyzing the scenarios simulated for this paper. The scenarios are schematized in Figure 2 (as mentioned, the mathematical formalization of the ABM is not detailed in this paper).

2.2.1 Main input data and parameters

i. Food-processing plant

The configuration of the multi-room meat-processing plant presented in this study was implemented based on our observations and investigations of industrial facilities. Such implementation can be easily adapted to any other user-defined configuration (additional rooms, production lines and/or equipment) by adapting the source codes provided with the paper. The dimensions of the meat-processing plant simulated herein (schematized in Figure 2) were 21m x 26m x 5m (w x l x h). Several spaces were modeled, including a main cutting room with an arrival gate (for the arrival of the raw carcasses to be processed) and a connected cooling area (for the storage of the final product), as well as several annex spaces. In general, these annex spaces are not directly connected to the main cutting room but are still accessible through an entrance hall whose dimensions and structures may vary from one plant to another. The following spaces were modeled herein: a changing room (for workers) with a connected restroom area, an office space, and a waste area. The main cutting room was configured with two successive conveyor belts located at the center of the room as well as packaging equipment located at the end of the second conveyor. Such configuration enabled the forward successive meat-processing steps, comprising the cutting steps, packaging, and storage (for more details on the dimensions of these objects, spaces, and their respective ventilation characteristics, see *online model description, section Food-processing plant*).

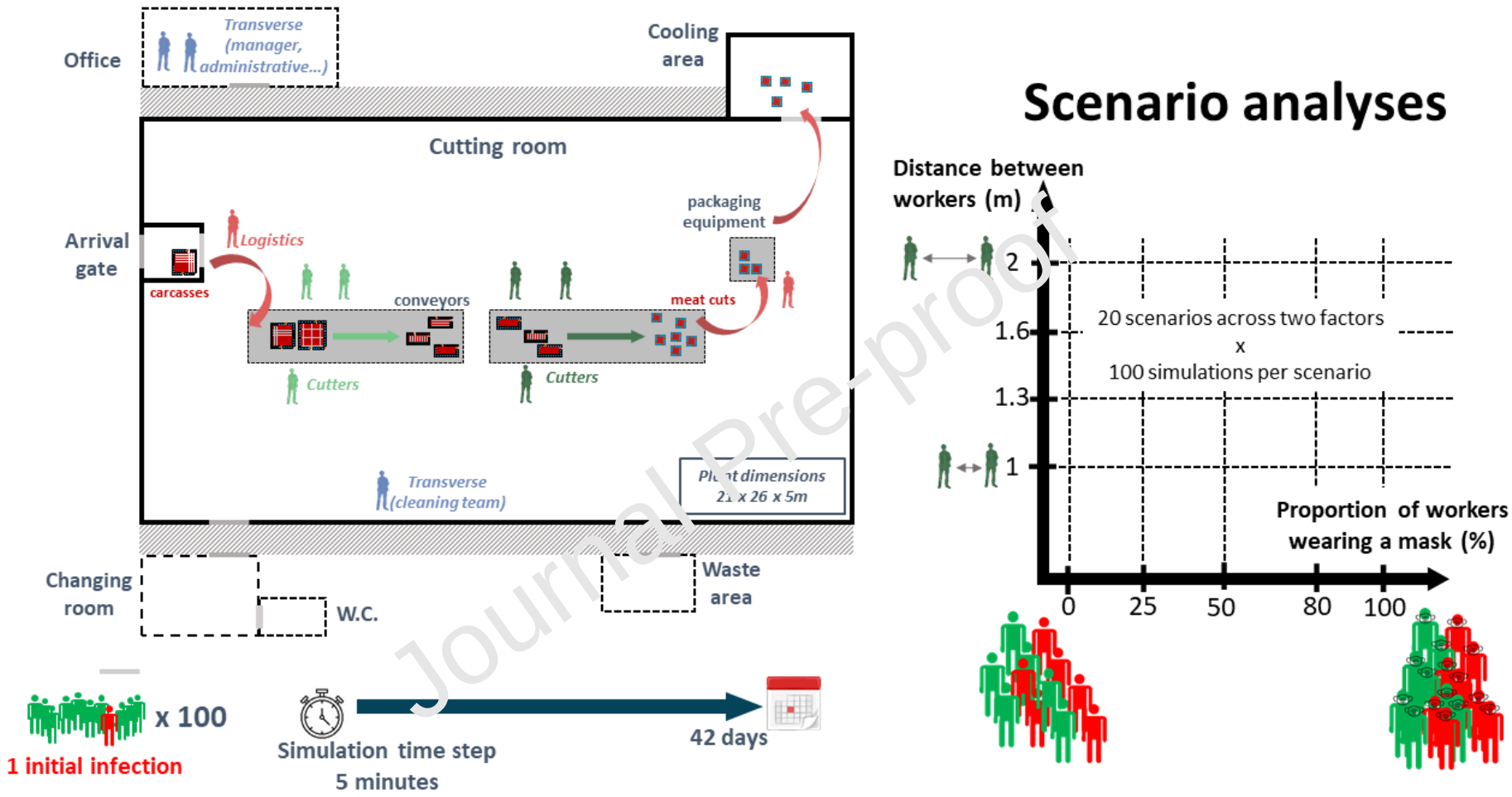

Figure 2 - Illustration of the modeled meat-processing plant and schema of the scenario analysis

ii. Workers

In our simulation, a total number of 100 workers were considered, with pre-defined proportions for the different worker types, estimated from preliminary studies and the literature. Three worker types were considered: (i) *cutters* (83%), especially located around the conveyors during their working day, in charge of carrying out the different processing/cutting steps (deboning, etc.) (Günther et al., 2020; Mallet et al., 2021); (ii) *logistics* workers in charge of transporting meat products between different areas of the plant (Günther et al., 2020; Mallet et al., 2021); and (iii) *transverse* workers, in other words the administrative staff, quality-control managers, or workers from the cleaning team (Mallet et al., 2021). These workers were attributed to different teams according to their working shift as well as their daily and weekly schedule. Based on industrial investigations, in order to ensure the continuity of the production lines, the working schedule considered possible team overlaps and team changes between different types of workers in case of absences (*cf. online model description, sections Type of workers, Working days and schedule*).

iii. Air

Based on data obtained by Buonanno et al. (2020), the ABM model considered six size classes of the droplets with the midpoint diameters between 0.8 and 100 µm. In each room, depending on the size and airflow conditions, the droplets were considered in two groups: (i) those being aerosolized (small droplets in rooms with high air velocities), and (ii) those directly contaminating other workers or falling directly on the surfaces around the emission source (large droplets in rooms with low air velocities). For the aerosolized droplets (group i), the evolution of the contaminated-droplet concentration in the air of each room between two successive time points was computed by accumulating the contaminated droplets exhaled by infectious workers and removing the ones inhaled by other workers, sedimented on surfaces/food, or lost via the air-renewal system. The concentration of aerosolized droplets was assumed to be homogeneous in the room, therefore implying the distance from the source (infectious worker) regarding the exposure to aerosolized droplets (group i) in the room had no

impact. For the large droplets in rooms with low air velocity (group ii), the effect of the distance from the source was taken into account with droplets that contaminated the workers and surfaces around the source (more details are provided in the *online model description, section Air*).

iv. Exposure pathways and dose response

The model considered two sources of worker contamination. The first was the exposure to SARS-CoV-2 linked to their respiratory activities inside the food-processing plant. The total number of SARS-CoV-2 particles inhaled by each worker was computed at the end of each working day. For each worker, the dose-response relationship developed by Watanabe et al. (2010) was then used to estimate the probability of becoming infected knowing the exposure. The second contamination source considered related to possible infections outside the plant by taking into account the local COVID-19 epidemic situation (regional/national incidence) and socio-community activities of the workers (for more details on the parameters characterizing the two sources of infection, see the *online model description, sections Infection probability, Dose-response parameters*).

v. Infection phases

The duration of the different infection phases was taken into account in the model. In summary, once infected, individuals first enter a pre-symptomatic phase that comprises: (i) a latent period lasting approximately 3.3 days during which no virus can be detected (Zhao et al., 2021), and (ii) a period of 2 days during which individuals become infectious before symptom onset (Byrne et al., 2020; Lau and Leung, 2020). At the end of the pre-symptomatic period, a proportion of the individuals will develop symptoms. Based on several studies from the literature, the proportion of asymptomatic individuals was estimated to be 33.5% (Alene et al., 2021; He et al., 2021; Ma et al., 2021; Sah et al., 2021). The duration of this symptomatic period was estimated to be about 8 days (van Kampen et al., 2021). From symptom onset to recovery (negative RT-PCR tests), a period of approximatively 13 days can be considered (Byrne et al., 2020). Possible absences of the workers from work were also taken into account in the model, since these absences could have direct influence on viral transmission and

potential production losses at the plant. For that, the model considered that the symptomatic workers had a probability of being absent from work (arbitrarily set at more than 80% herein) during a predefined period of absence fixed by health authorities.

vi. Inert surfaces and food portions

In our study, the different surface agents were defined as the $1m^2$ tiles that make up the surfaces of the equipment present in the plant (conveyors and packaging machine). On working days, SARS-CoV-2 infectious particles could accumulate on these surface tiles during the different time steps. This accumulation was due to possible droplet sedimentation from the air, projection by nearby workers through their respiratory activities/symptoms, or transfer from other food portions (Duret et al., 2017) transported from one location to another in the plant. Due to the lack of data from the literature, this accumulation of infectious particles was estimated by considering a ratio over the accumulation of viral RNA copies (Miller et al., 2020; Pitol and Julian, 2021). At the end of the day, a balance of this accumulation of SARS-CoV-2 particles was computed for each surface tile. Since it was assumed all surfaces were cleaned and disinfected at the end of each day, the number of SARS-CoV-2 infectious particles of each tile was reset to zero.

The different food agents were defined by all final food portions processed in the plant, generated daily depending on the number of workers present. Several spatiotemporal rules were implemented for describing the meat-cutting process from carcass to final product, thus providing the movements and locations of the different food portions at the different time steps (see details in the *online model description, section Food – cutting process*). Therefore, with regard to the surfaces' tiles, it's possible SARS-CoV-2 particles can accumulate on food due to droplet sedimentation, projection, or transfers between inert surfaces and food by contact (*online model description, section Transfers by contact*).

2.2.2 Computing

All the parameters' values included for the simulations are detailed in *Supplementary materials (Table S1)*. It is worth noting that, for a given scenario with a predefined set of input parameters, the output

results could differ from one simulation to the next because of the different stochastic parameters. The model was implemented entirely under an R environment (R Core Team, 2022). A convergence analysis was carried out for one reference scenario to determine the required number of simulations and thus obtain credibility intervals associated with output results. The convergence of the model was estimated at about 100 simulations per scenario. Since the computing time could be significant for each scenario due to an important number of simulations, the latter were performed in parallel using an online R platform (Migale, 2020), migale.inrae.fr). All source codes for model implementation can be found on Github (github.com/ndmluong/sacada).

2.2.3 Scenarios

In this paper, the scenario analysis aimed to study the potential effects of taking two preventive measures with regard to viral transmission: raising the mask-wearing proportion of workers and increasing the physical distancing between them. The considered proportions of mask-wearing among the workers were 0, 25, 50, 80, and 100%. The physical distancing was artificially implemented in the model by increasing the length of the conveyors present in the plant and then varying the distances between the workers located around these conveyors. In our scenario analysis, the distances between workers were computed from approximately 1m to 2m by varying the length of the conveyors from 11m to 20m in the simulated plant configuration. In total, 20 scenarios were considered according to combinations across the two measures above (cf. Figure 2). The scenarios illustrated in this paper was simulated for facilities processing pork meat with a theoretical production capacity of the 100-person plant estimated at around 2000 processed carcasses in total per day, which was very close to our observations in industrial facilities. All simulations were carried out according to the situation in 2020 by setting parameters characterizing the original variant of concern, while all workers were assumed to be susceptible to the virus. For each scenario, 100 independent simulations were performed ($N_{sim} = 100$) with five-minute time steps and for a total duration of 42 days ($N_{days} = 42$). For all the

scenarios mentioned above, the model was initialized with one infected worker on the first working day, corresponding to the first infection source.

2.3 Output indicators

The contamination of the workers, inert surfaces, and food was determined daily and/or during the overall 42-day period by estimating several numeric indicators. Below, we provide some indicators extracted from our scenario analysis.

Worker contamination

The number of newly infected workers was calculated daily for each performed simulation, thus giving the different epidemic curves corresponding to each simulation. Based on these new daily infections, the cumulative number of infected workers was calculated over time and at the end of the 42-day period. It is worth noting that, for each scenario, despite the same initializing point, the shape of the epidemic curves can be completely different from one scenario to the next due to the probabilistic model parameters. To illustrate this point, for the same given scenario, the cumulative number of infections after 42 days can be 16, 35 or 45 workers in three different simulations. Based on the criteria of French national epidemiological investigations, a cluster was defined by the occurrence of at least three cases during a seven-day period. However, after the first lockdown period in 2020, because of the quickly increasing number of infection cases, the local Regional Health Agencies were instructed to prioritize their investigations. In the framework of our overall research project, a minimum cumulative number of 25 infected workers was chosen, since this threshold value enabled us to obtain mostly exhaustive information in terms of investigations that would be useful for further comparison purposes. For this reason, in this paper, we defined the occurrence of a cluster situation (respectively a non-cluster situation) when it presented at least 25 cases (respectively fewer than 25 cases). Thus, for each scenario, denoted S, the cluster-occurrence probability was estimated as the ratio between the number of simulations giving at least 25 infected workers and the total number of performed

simulations: $prob_{cluster,S} = \frac{n_{sim(\geq 25\ infections),S}}{N_{sim}}$. Since the different infection phases were integrated in the model (from newly infected to recovered), the simulated epidemic curves over the 42-day period can be shaped with an increasing phase followed by a decreasing one. The peak values of each curve, expressed at the highest daily number of infected workers during the simulated period, can once again be more or less important from one simulation to the next. These peak values were estimated and are discussed below, both for situations that present a cluster occurrence and those that do not.

Surface contamination

As mentioned above, the surface agents were defined as the different 1m^2 tiles that make up the surfaces of the equipment present in the plant (conveyors and packaging equipment). In our study, each surface tile was considered contaminated at the end of a given day if the number of SARS-CoV-2 particles that had accumulated on it exceeded a threshold value equivalent to 5 $\log_{10}$ RNA copies. This accumulation of viral particles was due to possible droplet sedimentation and projection or transfers. For a given day, the surface contamination, expressed in %, was defined as the ratio between the number of surface tiles exceeding the contamination threshold above and the total number of surface tiles in the plant. Since all surfaces were assumed to be cleaned and disinfected daily, for a given simulation, the overall surface-contamination indicator during the simulated period was estimated by averaging the daily values across all working days (weekend days were not considered).

Food contamination

As for surface contamination, the same threshold value of 5 $\log_{10}$ RNA copies was chosen for the equivalent of food contamination by SARS-CoV-2 particles. For a given day, the food contamination, expressed in %, was defined as the ratio between the number of food portions exceeding this threshold and the total number of food portions processed during the day in question. The overall food-contamination indicator during the simulated period was estimated by averaging the daily ratio values across all working days (weekend days were not considered).

It is worth noting that the possible absences of one or more workers from work can directly influence the total quantity of processed food. Therefore, we also introduced a metric to estimate possible losses regarding production by the plant. For a given simulated period, this metric, expressed in %, was defined as the ratio between the total quantities of processed food on the days when workers were most absent and when they were most present (equivalent to the maximum amount of food produced daily by the plant). This metric enabled us to estimate the amplitude of production losses between these two most extreme days.

3 Results

The developed ABM was computed to study the effects of preventive measures with regard to the contamination of workers, surfaces, and food products in a meat-processing plant. Several parameters were defined, as presented in previous sections, to establish illustrative scenarios of a typical food-processing-plant operation. The results presented below correspond with the analysis of 100 simulations per same scenario.

3.1 Worker contamination

3.1.1 Cumulative number of infections after 42 days

Starting with one infected worker (out of 100) from the first day, the distribution of the cumulative numbers of infections after the 42-day simulation period in every scenario is described in Table 1. On average, the highest cumulative number of infections was estimated to be about 50 out of 100 workers and seemed to be associated with the scenarios in which no or few workers were wearing a mask. In contrast, the lowest average cumulative number of infections was observed in scenarios with the maximal mask-wearing ratio (100%) and was estimated to be about 6 infected workers (out of 100).

Table 1 - Cumulative number of infections after 42 days depending on the mask-wearing ratio and the distance between workers: average values and distribution (5% quantile, median values, 95% quantile, *maximum values*). The total number of workers considered for each simulation: N = 100. The highlighted cases correspond to the three situations with the highest cumulative number of infections (average across simulations)

Mask-wearing (%) **Distance between workers**	**0%**	**25%**	**50%**	**80%**	**100%**
1 m	**57** [1; 84; 99; *100*]	**53** [1; 72; 98; *99*]	**30** [1; 7; 94; *99*]	**18** [1; 5; 80; *90*]	**6** [1; 4; 16; *38*]
1.3 m	**56** [1; 82; 100; *100*]	**44** [1; 11; 98; *100*]	**31** [1; 7; 95; *99*]	**16** [1; 6; 64; *86*]	**5** [1; 4; 16; *32*]
1.6 m	**47** [1; 18; 100; *100*]	**44** [2; 17; 97; *100*]	**31** [1; 8; 94; *96*]	**13** [1; 5; 67; *80*]	**6** [1; 4; 14; *48*]
2 m	**45** [1; 12; 99; *100*]	**40** [1; 12; 98; *100*]	**26** [1; 6; 93; *98*]	**11** [1; 5; 41; *81*]	**6** [1; 4; 18; *46*]

Considering the full distribution of the estimated cumulative number of infections in every scenario, an important difference was observed between the average (in bold) and the median (underlined) values (Table 1). These observations could probably be associated with the fact that, for a same given scenario, some simulations could provide an exceptionally high (or low) cumulative number of infections unlike the other ones providing much fewer (or more) infections. It is interesting to note the distribution of cases over the 100 simulations generated for the three highlighted situations (0% or 25% mask-wearing with a distance of 1m and 0% mask-wearing with a distance of 1.3m): the median values were very high, indicating that 50% of simulations generated more than 72 cases after 42 days.

It would also be interesting to study the amplitude of the epidemic curve in order to gain insights into the maximal number of infected workers at the same given time point. The distribution of the peak values observed in the epidemic curves across the different simulations are provided in Supplementary materials (Supplementary materials, Figure S1). In situations with more than 25 cases, increasing the mask-wearing ratio had an effect on the amplitude of the peak, which decreased from about 80 infected workers to a peak close to 25. In the cases of fewer than 25 cumulative infections after 42 days, whatever the scenarios, the epidemic peaks very rarely exceeded 6 infections (Supplementary materials, Figure S1). Overall, no clear effect of the distance between the workers in the plant was graphically observed on the intensity of the peak.

3.1.2 Cluster-occurrence probability

The probabilities of observing a cluster with at least 25 infections estimated from the simulations depending on the mask-wearing ratio and the physical distancing are plotted in Figure 3. On the one hand, the highest probability of occurrence was estimated to be between 43% and 61% and observed in the situation where no workers wore a mask. In this situation, the occurring clusters also presented peak values at mainly more than 80 infected workers (Supplementary materials, Figure S1). On the other hand, the situation where all workers wore a mask (100%) presented the lowest cluster-occurrence probabilities, all estimated at less than 3%. Globally, increasing the mask-wearing ratio could lead to an observable decrease in cluster-occurrence probability, no matter the distance between the workers. The influence of physical distancing was not clearly observed for all situations. However, in the cases where no or few workers wore a mask (0% or 25% of mask-wearing ratio), increasing the average distance between two workers from less than 1m to more than 2m decreased the cluster-occurrence probability by up to 15%.

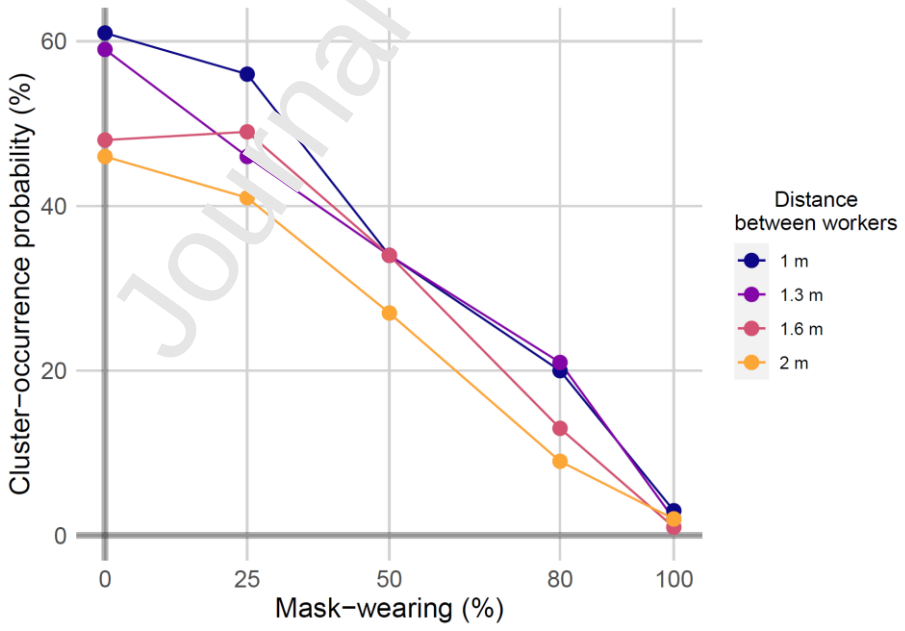

Figure 3 – Cluster-occurrence probability depending on the mask-wearing ratio and the physical-distancing measure (artificially implemented by varying the length of the conveyors). The mask-wearing ratio was expressed as the proportion of the present workers wearing a surgical mask. The minimal (resp. maximal) distance between workers was set at about 1m (resp. 2m) by computing the conveyors' lengths at 11m (resp. 20m) in the simulated configuration. The probability estimated for each scenario was expressed as the ratio between the number of simulations, giving at least 25 infections and the total number of simulations per scenario (N = 100)

3.1.3 Production losses

Loss of food-production capacity was a direct consequence of the workers' contamination, especially in cluster situations, since their absence from work during a given period led to a decrease in the total number of processed food portions. The metric used compares the production of a normal working day (with the most present workers) with the one with the highest number of absences related to COVID-19 over the simulated period of 42 days. The comparison of these potential losses between the cluster and non-cluster situations is graphically represented in Figure 4. In non-cluster situations (fewer than 25 infections), the estimated production-capacity metric seemed stable at about 83%-85% on average, suggesting a potential reduction of about 15% of the regular production capacity due to absences, no matter the mask-wearing ratio and the distance between the workers. In contrast, in the scenarios without mask-wearing and leading to cluster occurrence, the metrics were estimated at less than 60%, corresponding to potential losses of more than 40% of the production capacity compared to regular working conditions. No clear direct influence of the physical-distancing measure was graphically observed on the production capacity; however, once again, increasing the mask-wearing ratio seemed globally to maintain the production capacity at optimal levels.

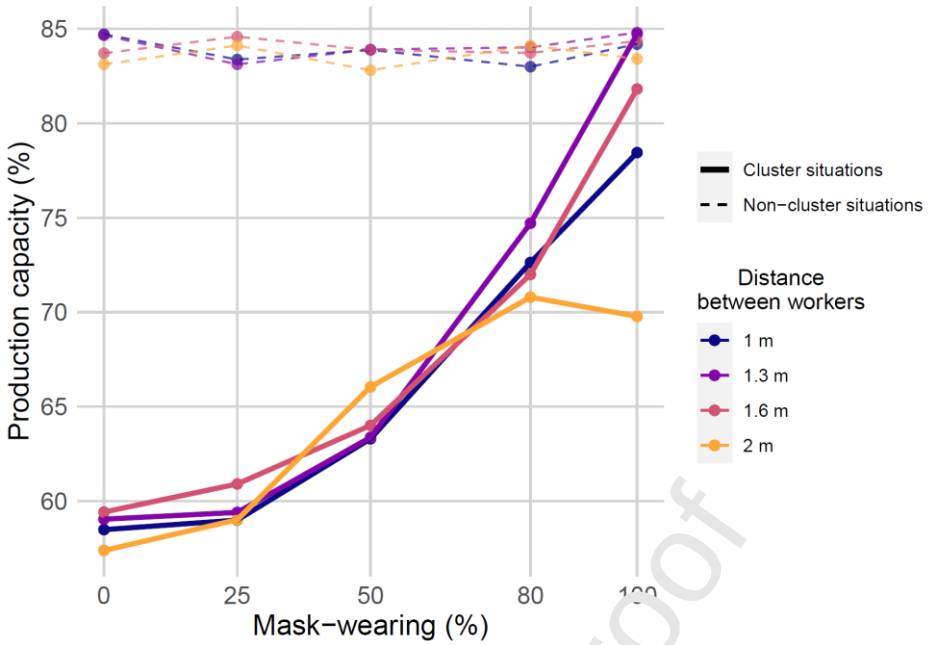

Figure 4 – Production-capacity metric depending on the mask-wearing ratio and the physical-distancing measure, in cluster (thick lines) and non-cluster (dotted lines) situations (presenting more and fewer than 25 infections, respectively). For a given simulation, the production capacity of the simulated period, expressed in percentage, was defined as the ratio between the quantities of processed food on the days with the most absent workers and those with the most present workers. Points: average values across different simulations. The minimal (resp. maximal) distance between workers was set at about 1m (resp. 2m) by computing the conveyors' lengths at 11m (resp. 20m) in the simulated configuration

3.2 Contamination of inert surfaces and food

3.2.1 Surface contamination

As described in the previous sections, the considered surfaces herein corresponded to the $1m^2$ tiles that make up the inert surfaces of the equipment present in the plant, including the conveyors and the packaging machine. Each surface tile was defined as being contaminated by SARS-CoV-2 particles if it exceeded an equivalent value of 5 $\log_{10}$ of viral RNA copies accumulated at the end of the working day. The distribution of average surface contamination across the simulated 42-day period depending on the mask-wearing ratio and the physical-distancing measure is plotted in Figure 5.

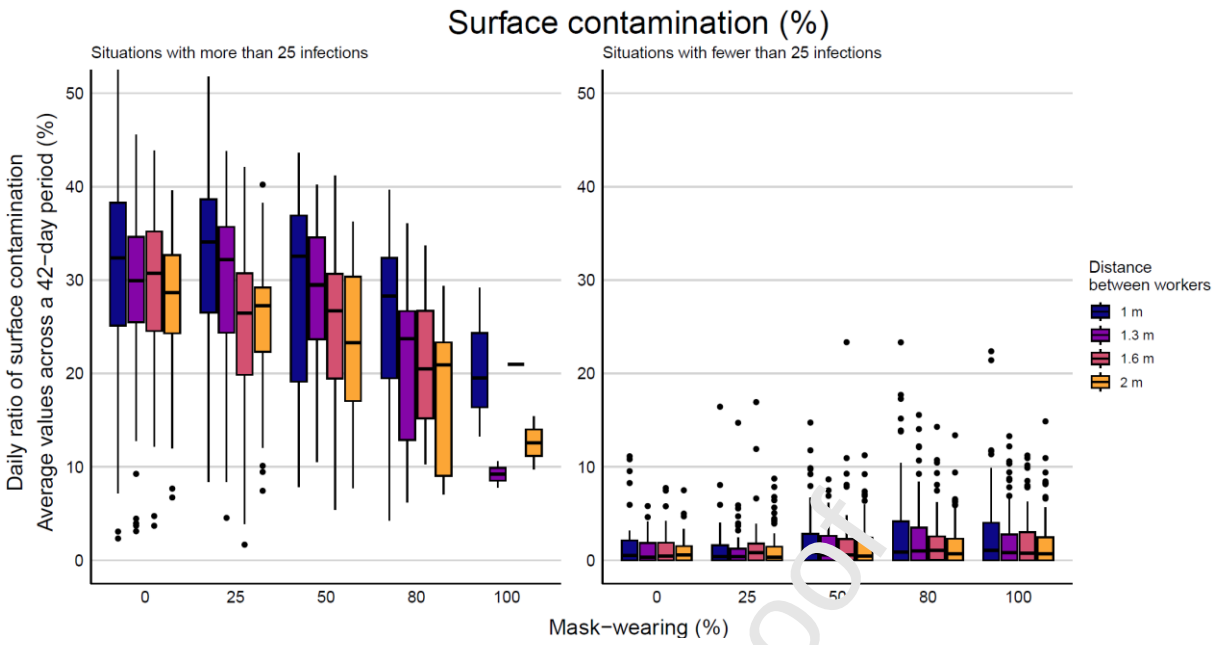

Figure 5 – Distribution of the average daily surface contamination depending on the mask-wearing ratio and the physical-distancing measure for simulations presenting more (left) and fewer (right) than 25 infections. The box represents the values between the 1st and 3rd quartiles of the distribution. The daily surface contamination, expressed in %, was defined as the ratio between the number of surface tiles exceeding the contamination threshold (5 $\log_{10}$ of viral RNA copies) and the total number of surface tiles in the plant. The minimal (resp. maximal) distance between workers was computed at about 1m (resp. 2m) by computing the conveyors' lengths at 11m (resp. 20m) in the simulated configuration.

As shown in Figure 5, a considerable difference in the surface contamination was observed between the cluster and non-cluster situations (more and fewer than 25 infections after 42 days, respectively). Considering the equivalent contamination threshold fixed at 5 $\log_{10}$ of viral RNA copies per m^2, in the case of cluster occurrences, the daily surface contamination might reach in median more than 30% of the overall surfaces if no worker wore a mask in the plant. The contamination was likely reduced with the increase of the mask-wearing ratio. With a mask-wearing ratio of 100%, this contamination was estimated at less than 20% in the rare situations of cluster occurrences ($n \leq 3$, cf. Figure 5). In non-cluster situations, the observed daily surface contamination remained at a very low level, no matter the mask-wearing ratio and the distance between workers. Indeed, despite several observed outlier points in the boxplots corresponding to these situations shown in Figure 5, the contaminations were all estimated as being below 3% in median, with narrow interquartile value ranges.

3.2.2 Food contamination

The food portions present in the plant were modeled as agents of the ABM following several successive processing steps (transport, meat-cutting steps, packaging, and storage). The contamination of each food portion was computed at its final step, i.e. storage in the cooling area, as results of accumulation of viral particles on it due to sedimentation and projection of droplets, as well as possible transfers from other contact surfaces. As for the inert surfaces, a food portion (meat cut) was defined as contaminated by SARS-CoV-2 particles if it presented at least an equivalent value of 5 $\log_{10}$ of viral RNA copies. The distribution of average daily food contamination across the simulated 42-day period is plotted in Figure 6, for both cluster and non-cluster situations.

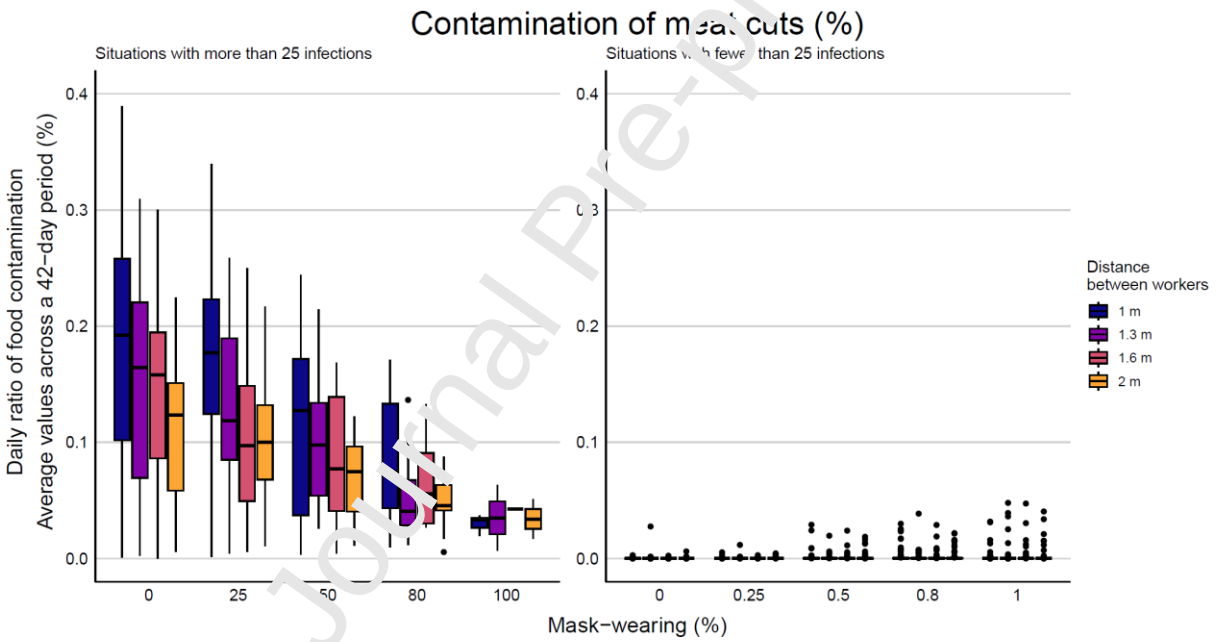

Figure 6 – Distribution of the average daily food contamination depending on the mask-wearing ratio and the physical-distancing measure, for simulations presenting more (left) and fewer (right) than 25 infections. The box represents the values between the first and third quartiles of the distribution. The food contamination at a given day, expressed in %, was defined as the ratio between the number of food portions (meat cuts) exceeding the predefined contamination threshold (5 $\log_{10}$ of viral RNA copies) and total number of processed-food portions of the day, varying depending on the number of present workers. The minimal (resp. maximal) distance between workers was computed at about 1m (resp. 2m) by computing the conveyors' lengths at 11m (resp. 20m) in the simulated configuration

Similar patterns in food contamination were observed for the surfaces, especially concerning the great difference between the cluster and non-cluster situations. In cluster situations, the most notable daily food contamination was estimated at about 0.19% in median value and 0.39% as the maximum. This contamination level corresponded to the worst-case scenario, which had no worker wearing a mask, a

distance of 1m between workers, and presented more than 80 workers observed at the infection peaks (Figure 6, Supplementary materials Figure S1). As for the surfaces, increasing the mask-wearing ratio led to a great reduction in food contamination: when all workers wore a mask, the food contamination was estimated to be about 0.03-0.04%. In cluster situations, the distance between employees enabled a reduction in the number of contaminated food portions, particularly with a low mask-wearing ratio (0-25%). Finally, in the case of non-cluster situations (fewer than 25 infections), food contamination remained at very low levels, estimated to be, on average, less than 0.002%, no matter the mask-wearing ratio and the distance between the workers.

4 Discussion

Within the framework of good hygiene practices at food processing premises and food-safety culture during the COVID-19 pandemic, this paper aimed to better understand the potential effects of management measures on the transmission of SARS-CoV-2 using a simulation-based approach. The studied measures, which included mask-wearing and physical distancing, were chosen as illustration for our simulations because of their simple practical implementation in food-processing plants and their wide application during the pandemic in closed environments. The developed ABM took place in a global research project, and so enabled the inclusion of many input data and parameters. These were collected from the literature and multiple investigations in order to outline the different characteristics related to the plant and the virus, and to be as close as possible to realistic conditions. Our simulation-based approach also enabled us to define several output indicators for simultaneously monitoring the contamination of the workers, surfaces, and food portions processed in the plant in different scenarios. Studying scenarios was also facilitated, since the model was implemented using generic structures, thus providing flexibility for user-defined changes in one or several input parameters of interest.

As illustrated by the simulations shown in this paper for a given *typical* meat-cutting plant, unsurprisingly the results pointed to the influence of the mask-wearing ratio on viral transmission.

Increasing the mask-wearing ratio in the plant led to a great reduction in the probability of observing a cluster, and in the case of clusters, a reduction in the contamination of inert surfaces and food portions and maintenance of the plant's production capacity at optimal levels. The similar patterns observed in surface and food contamination were also expected, since these two modules were intimately linked due to transfer between contact surfaces, as well as similar possible interactions with the air in the plant caused by, for example, droplet sedimentation and/or projection. Only a slight reduction in the risk of infection was observed when the distance between workers was increased from 1m to 2m. The results of our study also suggested that increasing the distance between employees reduced the incidence of contamination of food products for a low mask-wearing ratio during cluster situations.

The relative effects of the two measures tested in our study were quite consistent with the findings in the literature, in particular the effects of mask-wearing on the decrease of infections. A meta-analysis on epidemiological measures conducted by Chu et al. (2020) has pointed to a great reduction in the risk of infection, estimated at 14.3%. The authors also observed only a slight reduction in the risk of infection when increasing the distance between individuals from 1m to 2m, as observed in our simulations.

The literature has mentioned reductions in activities, or even closures, of several processing plants or food facilities due to cases (epidemics) among their staff and problems relating to absences. These partial or total closures had consequences on the entire value chain, both upstream in terms of supply flows, and downstream on food retailers and supply volumes (Hobbs, 2021; Pokora et al., 2021; Weersink et al., 2020). Our simulations showed there could be a high rate of absences, and thus a possible loss of production, between the two most extreme days (Figure 4). The metric used herein enabled a scenario comparison between two days, independently, and illustrated an influence on the economic loss by absences. Hence, this metric can allow us to identify the situations where the loss of production will be the most critical between two days compared to the normal situation. For further

studies, it would also be interesting to define other metrics, for example to characterize the effects on the cumulative lost production over the total duration of the epidemic period compared to the normal situation.

The low ratios in the presence of viral RNA on food and surfaces simulated by the model were quite expected in view of some data reported in the literature. A study by Li et al. (2022) registered 1,398 food samples as positive for SARS-CoV-2 nucleic acid out of 20,517,959 tested food samples, corresponding to a ratio of 0.007%. Ming et al. (2021) found that 1.23% (278 of 22,643) of the total environmental samples collected in food-processing plants were SARS-CoV-2 positive, which was close to our estimated surface-contamination ratio in non-cluster situations (about 1-3%; Figure 6). Ming et al. (2021) also reported a particular case associated with an establishment monitored during the period March to September 2020, when restrictions like mask wearing or quarantine were applicable. This establishment presented a positive result for 10.1% human samples (of 1,248 collected) and 9.2% environmental samples: this positivity corresponded strongly with our simulations in some rare cases, where the mask-wearing ratio was at 100% presenting more than 25 infections (Figure 5).

The simulated results did not show clear influence of the physical-distancing measure for all the estimated indicators. At first sight, this measure seemed to reduce surface and food contamination. However, one should interpret these observed reductions with caution. It is worth remembering that, in this paper, the distancing measure was artificially implemented by varying the length of the conveyors in the plant. The contamination ratio for the inert surfaces and food by transfer was determined based on the total surface. Thus, a reduction in the contamination ratio while increasing the conveyor length might be associated not only with the effects of the measure but also with a "dilution" effect simply due to the implemented numerical formalization. However, the choice to vary the length of the conveyors for artificially modeling the physical-distancing measure was made in order to maintain the same total number of workers across the different scenarios. Finally, the fact that the effects of the distancing measure were not clearly observed might also be due to an insufficient

variation amplitude between the tested lengths of the conveyors. In this paper, these lengths were computed at 11 and 20m, corresponding to about 1m and a little more than 2m between two workers in the simulated plant configuration, respectively. Increasing these hypothetical lengths to more than 20m might not be appropriate or realistic for simulations, especially due to constraints on the dimensions of the plant, fixed at 21m x 26m, as shown in Figure 2, based on observations and investigations. All the constraints mentioned above might therefore explain the encountered difficulties in simulating and studying the effects of physical distancing on viral transmission. For further studies, it would also be interesting to simulate other workforce-management measures, such as placing barriers between workers. Such implementation is possible by adjusting the input parameters characterizing the spatial distribution of droplets emitted by infectious workers to nearby environments.

In this paper, based on the different simulations performed, several indicators were estimated to describe the contamination of the workers (e.g. the cumulative number of infections after 42 days, infections peaks, and cluster-occurrence probability). Other indicators could also be calculated without having to repeat any simulations: one can cite, for example, the effective or initial transmission rate, widely used in the epidemiological study framework. The calculation of these rates was also carried out herein (results not shown). However, for some simulations, the estimations were not always numerically possible and could present considerable uncertainty ranges, leading to difficulties with comparison between scenarios. Unlike large-scale epidemiological studies in the literature (generally at population or meta-population scales), the number of infections observed in our illustrative simulations did not seem high enough to obtain plausible estimations of the transmission rates (fewer than 100 workers during a 42-day period). Wide uncertainty ranges associated with estimation of the transmission rates have been already identified in the literature, e.g. the study proposed by de Laval et al. (2022). Therefore, considering viral transmission in relatively small and closed environments such as food-processing plants could be interesting for scenarios with a greater population size or a longer

simulation period, although that might require additional methodological adaptations for the estimation step.

Surface and food contamination by SARS-CoV-2 particles was presented in this paper using an equivalence of a contamination-threshold value fixed at 5 $\log_{10}$ of RNA copies per unit of surfaces ($1m^2$). This level was set based on the expected limit of detection (LOD) for experiments on surfaces: Parker et al. (2020) estimated the LOD at 1,000 viral particles per $25cm^2$, corresponding to a limit of between 5 and 6 $\log_{10}$ particles per m^2. In this paper, the model was implemented in a way whereby one can consider the contamination at different levels (from 3 to 9 $\log_{10}$ RNA copies) for any further potential adaptation purposes due to new LOD estimations. As for the contamination-threshold value discussed above, some other model parameters and assumptions were arbitrarily chosen for our illustrative scenario analysis, mainly due to the lack of data enabling plausible estimation for their values and the wide uncertainty ranges. One can cite, for example, the absence probability arbitrarily computed in this paper at more than 80% for the asymptomatic workers. The ratio between the quantity of the RNA copies and the infectious viral concentration was set at 500 according to existing hypotheses used in other risk-assessment studies but could present wide uncertainty ranges (Miller et al., 2020; Pitol and Julian, 2021). It is worth noting that such parameters might have a large influence on the simulated outputs. Thus, it would be interesting to perform supplementary analyses by considering the uncertainty ranges of these parameters in order to identify their potential influence and to better refine the model.

Although ABMs, as used in this study, provide the possibility to include several input data to get as close as possible to realistic conditions, simulations might require significant computing duration (several hours, days, etc., depending on the time step, periods, and number of simulations per scenario). Thus, parallel computing using an online server was necessary in this project to perform the simulation for the different considered scenarios as well as other preliminary tests and convergence analyses. These computing jobs were done in a way that meant every simulated characteristic for every

agent could be stored, thus enabling estimation *a posteriori* of the different contamination indicators/metrics of interest. Based on these obtained indicators summarizing the different scenarios, it would be interesting to implement a simplified empirical model focusing only on the indicators/input parameters of interest. Such a simplified model could represent a base for building a quick, ready-to-use simulation tool that would be helpful as a communication-support tool for professionals in the food-processing sector.

In this paper, we would like to illustrate our ABM approach for describing viral transmission in food-processing plants with a focus on food and surface contamination. In view of the discussion, we are convinced that the developed workflow can open up multiple perspectives in terms of refining the model, adjusting model parameters, reuse in other user-defined scenarios, and comparing simulations with epidemiological data. Exhaustively exploring the simulated results could enable identification of other transmission factors, such as the co-occurrence of superspreading events and high peaks of surface or food contamination. Finally, for further studies, validating the model illustrated herein using epidemiological data could undoubtedly be of primary interest. Collecting these epidemiological data combined with available information concerning the investigated food-processing plants (production capacity, size, preventive measures, etc.) could be undertaken for model-validation purposes in the estimation of cluster-occurrence probabilities at regional or national scales.

Funding sources

This research was funded by the French Research National Agency (ANR) within the framework of the SACADA Project (ANR-21-CO13-0001).

Acknowledgements

The authors are grateful to the collaborators from the SACADA consortium for their helpful comments and expertise in the fields of virology and food safety: Christophe Batéjat, Maxence Feher, Lisa Fourniol, Sophie Le Poder, India Leclercq, Jean-Claude Manuguerra, Moez Sanaa, Jessica

Vanhomwegen, Prunelle Waldman. The authors also thank Cyprien Guérin (MaIAGE) and the INRAE MIGALE Bioinformatics facility (Migale (2020), migale.inrae.fr) for providing helpful advice on carrying out parallel computing and online-storage resources.

Conflicts of interest

The authors declare no conflict of interest.

Authors contribution

- Conceptualisation: E. Chaix, S. Duret, L. Guillier, N.-D. M. Luong;
- Data curation: E. Chaix, S. Duret, M. Federighi, L. Guillier, Y. Guillois, P. Kooh, N.-D.M. Luong, A.-L. Maillard, M. Pivette, S. Martin-Latil;
- Formal analyses: E. Chaix, S. Duret, L. Guillier, N.-D. M. Luong;
- Funding acquisition : E. Chaix;
- Methodology: G. Boué, E. Chaix, S. Duret, L. Guillier, N.-D. M. Luong;
- Project administration: E. Chaix, S. Martin-Latil;
- Software: E. Chaix, S. Duret, L. Guillier, N.-D. Luong;
- Supervision: E. Chaix, S. Duret, L. Guillier, S. Martin-Latil ;
- Visualisation: E. Chaix, S. Duret, M. Federighi, L. Guillier, N.-D.M. Luong ;
- Writing – original draft: E. Chaix, S. Duret, L. Guillier, N.-D.M. Luong;
- Writing – review and editing: E. Chaix, S. Duret, M. Federighi, L. Guillier, Y. Guillois, P. Kooh, N.-D.M. Luong, A.-L. Maillard, M. Pivette, S. Martin-Latil.

All authors approved the final version of the manuscript.

Supplementary materials

- All source codes for model implementation can be found in Github (github.com/ndmluong/sacada).
- Supplementary materials – Figure S1:

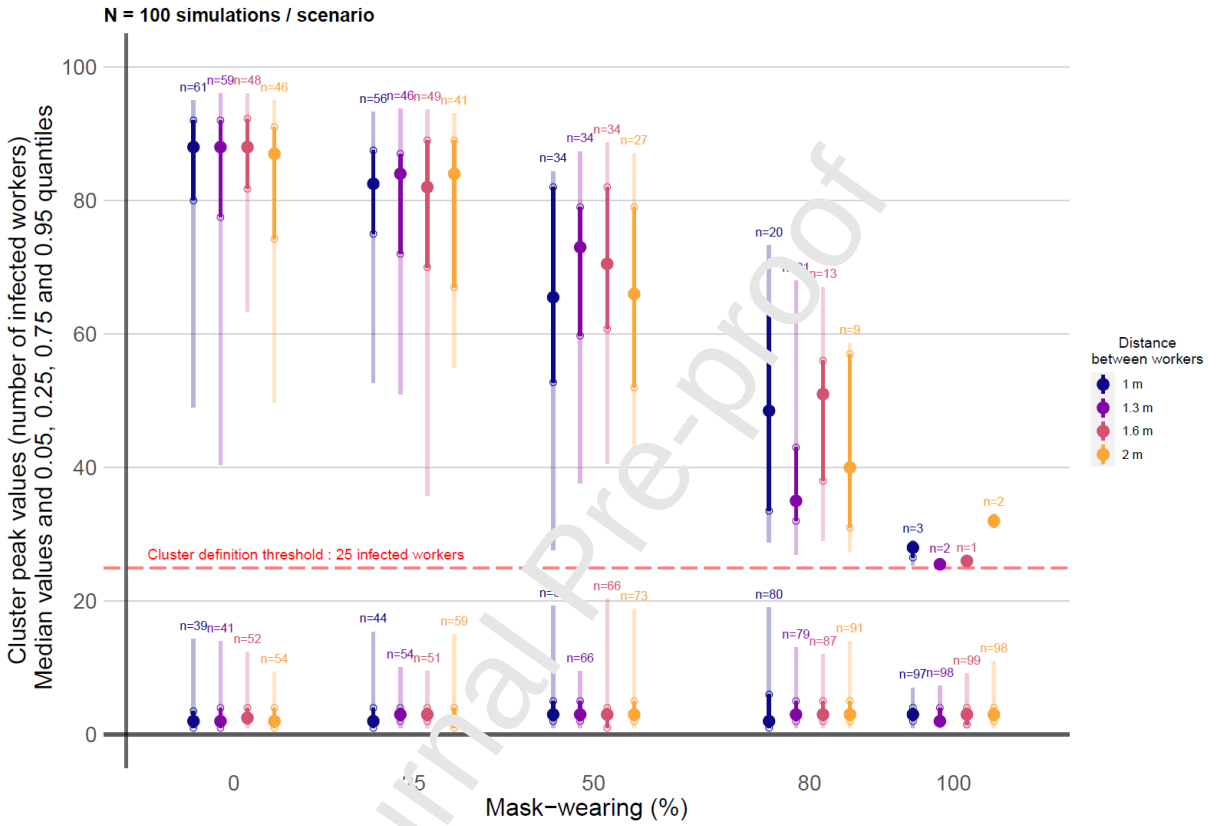

Figure S 1 – Distribution of the peak values of the observed epidemic curves (expressed as number of infected workers), depending on the mask wearing ratio and the physical distancing measure, for both simulations that presented more and fewer than 25 infections. Distribution of these peak values: the points correspond to the median, the bold lines correspond to the interquartile ranges, and the transparent lines correspond to the ranges between the 5% and 95% quantiles. The annotated values of n correspond to the number of simulations giving the cumulative number of infections of more or fewer than 25 infections after 42 days. The mask-wearing ratio was expressed at the proportion of the present worker wearing a surgical mask. The minimal (resp. maximal) distance between workers was computed at around 1m (resp. 2m) by computing the conveyors' length at 11m (resp. 20m) in the simulated configuration.

- Supplementary materials / Table S1 – Values of the model parameters used for scenario analysis

Definition		Unit	Value	References
Food processing plant				
Spaces				
Main cutting room	*width x length x height*	m	26 x 21 x 5	User-defined input
	air renewal rate	m^3/h	2400	Regulation
	air flow rate	m^3/h	90000	Assumption
Changing room	*width x length x height*	m	5 x 4 x 3	User-defined input
	air renewal rate	m^3/h	90	User-defined input
	air flow rate	m^3/h	90	User-defined input
Restroom	*width x length x height*	m	2 x 2 x 2.5	User-defined input
	air renewal rate	m^3/h	30	Assumption
	air flow rate	m^3/h	30	Assumption
Cooling area	*width x length x height*	m	5 x 5 x 3	User-defined input
	air renewal rate	m^3/h	120	Assumption
	air flow rate	m^3/h	500	Assumption
Arrival gate	*width x length x height*	m	2 x 2 x 3	User-defined input
	air renewal rate	m^3/h	30	Assumption
	air flow rate	m^3/h	200	Assumption
Waste area	*width x length x height*	m	2 x 3 x 3	User-defined input
	air renewal rate	m^3/h	30	Assumption
	air flow rate	m^3/h	200	Assumption
Office	*width x length x height*	m	5 x 4 x 3	User-defined input
	air renewal rate	m^3/h	120	Assumption
	air flow rate	m^3/h	200	Assumption
Objects				
Conveyor 1	*length*	m	**11; 14; 17; 20**	Input (scenarios)
	width	m	1	User-defined input
Conveyor 2	*length*	m	**11; 14; 17; 20**	Input (scenarios)
	width	m	1	User-defined input
Packaging equipment	*length x width*	m	1	User-defined input
Workers				
Total number of workers		# workers	100	User-defined input
Ratio of daily number of workers		ratio	1.25	French legislation
Proportion of each type of workers	*cutter1*	ratio	0.36	Mallet et al. (2021)
	cutter2	ratio	0.47	Mallet et al. (2021)

	logistic1	ratio	0.04	Gunther et al. (2020)
	logistic2	ratio	0.04	Mallet et al. (2021)
	transverse1	ratio	0.045	Mallet et al. (2021)
	transverse2	ratio	0.045	Mallet et al. (2021)
Workers proportion in teams	*team A*	ratio	0.5	Assumption
	team B	ratio	0.5	Assumption
Proportion of workers which change the team weekly		ratio	0.05	Assumption
Proportion of workers having community activities		ratio	0.21	Mallet et al. (2021)
Average number of workers per community		# workers	5	Assumption
Secondary attack rate (SAR)	*Unvaccinated – Original variant*	rate	0.17	Fung et al. (2021)
Daily secondary attack rate	*Unvaccinated – Original variant*	rate	0.017	Estimated from SAR
Mask type			surgical mask	User-defined input
Mask wearing ratio		ratio	**0; 0.25; 0.5; 0.8; 1**	Input (scenarios)
Mask efficacy		ratio	0.9	Assumption
Number of initial infected workers		# workers	1	User-defined input
Regional prevalence		rate	100/100000	User-defined input
Duration of the infection phases	*Latent phase*	day	3	Zhao et al. (2021)
	Pre-symptomatic	day	2	Byrne et al. (2020)
	Symptomatic	day	8	Byrne et al., (2020), van Kampen et al. (2021)
	Asymptomatic	day	8	Byrne et al. (2020)
	Non-infectious - Symptomatic	day	4	Byrne et al. (2020)
	Non-infectious - Asymptomatic	day	4	Byrne et al. (2020)
Probability of symptoms development		rate	0.335	Alene et al. (2021), Ma et al. (2021), Sah et al. (2021)
Probability to be absent if symptomatic		%	83	Arbitrarily set
Duration of the absence period		day	10	Fixed by health authorities
Air				
Droplet size classes (median size)		µm	0.8; 1.8; 3.5; 5.5; 20; 100	Buonnanno et al. (2020)

Droplet concentration through activities (for different size classes respectively)	*Breathing*	cm^{-3}	0.084; 0.009; 0.003; 0.002; 0; 0	Morawska et al. (2009), Kenedy et al. (2020)
	Voice counting	cm^{-3}	0.236; 0.068; 0.007; 0.011; 0; 0	Morawska et al. (2009), Kenedy et al. (2020)
	Unmodulated	cm^{-3}	0.751; 0.139; 0.139; 0.059; 0; 0	Morawska et al. (2009), Kenedy et al. (2020)
	Coughing	cm^{-3}	0.025; 0.145; 0.48; 2.51; 6.65	Duguid (1946)
	Sneezing	cm^{-3}	0; 13; 80; 175; 230; 489	Duguid (1946)
Respiratory rate depending on working activities	*Resting*	m^3/h	0.49	Adams (1993)
	Standing	m^3/h	0.54	Adams (1993)
	Light exercise	m^3/h	1.38	Adams (1993)
	Moderate exercise	m^3/h	2.35	Adams (1993)
	Heavy exercise	m^3/h	3.3	Adams (1993)
Symptoms frequency	*Coughing (infectious)*	occurrence/ min	0.003	Birrong et al. (2006)
	Coughing (symptomatic)	occurrence/ min	0.783	Birrong et al. (2006)
	Coughing (asymptomatic)	occurrence/ min	0.033	Birrong et al. (2006)
	Sneezing (infectious)	occurrence/ min	0.002	Hansen and Mygind (2002)
	Sneezing (symptomatic)	occurrence/ min	0.017	Musch et al. (2021)
	Sneezing (asymptomatic)	occurrence/ min	0.08	Hansen and Mygind (2002)
Droplets distribution from emission sources onto nearby locations (from the nearest to the farthest zones)	*same zone*	ratio	0.2	Estimation based on Li et al. (2021)
	adjacent zone 1	ratio	0.05	Estimation based on Li et al. (2021)
	adjacent zone 2	ratio	0.03	Estimation based on Li et al. (2021)
	adjacent zone 3	ratio	0.015	Estimation based on Li et al. (2021)
Droplets distribution from emission sources to exposed nearby workers (from the nearest to the farthest zones)	*same zone*	ratio	1	Estimation based on Li et al. (2021)
	adjacent zone 1	ratio	0.11	Estimation based on Li et al. (2021)

	adjacent zone 2	ratio	0.045	Estimation based on Li et al. (2021)
	adjacent zone 3	ratio	0.015	Estimation based on Li et al. (2021)
Surfaces				
Proportion of the surfaces tiles exposed to droplets	*inert surfaces*	ratio	1/3	Assumption
	meat cuts	ratio	2/3	Assumption
	number of exposed meat cuts	# portions	10	Assumption
Transfer rate	*from meat cuts to inert surfaces*	rate	0.99	Duret et al. (2017)
	from inert surfaces to meat cuts	rate	0.28	Duret et al. (2017)
Contamination threshold		# RNA copies	5 log	Miller et al. (2020), Pitol and Julian (2021)
Meat cuts				
Type of meat			porcine	User-defined input
Worker rhythm (porcine)	*porcine - logistic1*	carcasses/ min	1	Expert knowledge
	porcine - cutter1	carcasses/ min	0.2	Expert knowledge
	porcine - cutter2	carcasses/ min	0.1	Expert knowledge
	porcine - logistic2	carcasses/ min	0.5	Expert knowledge
Raw carcass weight (porcine)	*porcine*	kg	75	Expert knowledge / Data
Net weight ratio	*porcine*	ratio	0.59	Expert knowledge / Data
Consumer sales unit	*porcine*	kg	0.5	Assumption

References

Airoldi, A., Perricone, G., De Nicola, S., Molisano, C., Tarsia, P., Belli, L.S., 2020. COVID-19-related thrombotic microangiopathy in a cirrhotic patient. Dig Liver Dis 52, 946.

Alene, M., Yismaw, L., Assemie, M.A., Ketema, D.B., Mengist, B., Kassie, B., Birhan, T.Y., 2021. Magnitude of asymptomatic COVID-19 cases throughout the course of infection: A systematic review and meta-analysis. PLoS ONE 16, e0249090.

Backer, J.A., Mollema, L., Vos, E.R., Klinkenberg, D., van der Klis, F.R., de Melker, H.E., van den Hof, S., Wallinga, J., 2021. Impact of physical distancing measures against COVID-19 on contacts and mixing patterns: repeated cross-sectional surveys, the Netherlands, 2016-17, April 2020 and June 2020. Euro Surveill 26.

Bazant, M.Z., Bush, J.W.M., 2021. A guideline to limit indoor airborne transmission of COVID-19. Proc Natl Acad Sci U S A 118.

Buonanno, G., Morawska, L., Stabile, L., 2020. Quantitative assessment of the risk of airborne transmission of SARS-CoV-2 infection: Prospective and retrospective applications. Environ Int 145, 106112.

Byrne, A.W., McEvoy, D., Collins, A.B., Hunt, K., Casey, M., Barber, A., Butler, F., Griffin, J., Lane, E.A., McAloon, C., O'Brien, K., Wall, P., Walsh, K.A., More, S.J., 2020. Inferred duration of infectious period of SARS-CoV-2: rapid scoping review and analysis of available evidence for asymptomatic and symptomatic COVID-19 cases. BMJ Open 10, e039856.

Chaudhuri, S., Basu, S., Kabi, P., Unni, V.R., Saha, A., 2020. Modeling the role of respiratory droplets in Covid-19 type pandemics. Phys Fluids (1994) 32, 063309.

Chu, D.K., Akl, E.A., Duda, S., Solo, K., Yaacoub, S., Schünemann, H.J., Chu, D.K., Akl, E.A., El-harakeh, A., Bognanni, A., Lotfi, T., Loeb, M., Hajizadeh, A., Bak, A., Izcovich, A., Cuello-Garcia, C.A., Chen, C., Harris, D.J., Borowiack, E., Chamseddine, F., Schünemann, F., Morgano, G.P., Muti Schünemann, G.E.U., Chen, G., Zhao, H., Neumann, I., Chan, J., Khabsa, J., Hneiny, L., Harrison, L., Smith, M., Rizk, N., Giorgi Rossi, P., AbiHanna, P., El-khoury, R., Stalteri, R., Baldeh, T., Piggott, T., Zhang, Y., Saad, Z., Khamis, A., Reinap, M., Duda, S., Solo, K., Yaacoub, S., Schünemann, H.J., 2020. Physical distancing, face masks, and eye protection to prevent person-to-person transmission of SARS-CoV-2 and COVID-19: a systematic review and meta-analysis. The Lancet 395, 1973-1987.

de Laval, F., Chaudet, H., Gorge, O., Marchi, J., Lacrosse, C., Dia, A., Marbac, V., Mmadi Mrenda, B., Texier, G., Letois, F., Chapus, C., Garnier, V., Tournier, J.N., Levasseur, A., Cobola, J., Nolent, F., Dutasta, F., Janvier, F., group, P.-C.C.-i., Meynard, J.B., Pommier de Santi, V., 2022. Investigation of a COVID-19 outbreak on the Charles de Gaulle aircraft carrier, March to April 2020: a retrospective cohort study. Euro Surveill 27.

Duret, S., Pouillot, R., Fanaselle, W., Papafragkou, E., Liggans, G., Williams, L., Van Doren, J.M., 2017. Quantitative Risk Assessment of Norovirus Transmission in Food Establishments: Evaluating the Impact of Intervention Strategies and Food Employee Behavior on the Risk Associated with Norovirus in Foods. Risk Anal 37, 2080-2106.

Dyal, J.W., Grant, M.P., Broadwater, K., Bjork, A., Waltenburg, M.A., Gibbins, J.D., Hale, C., Silver, M., Fischer, M., Steinberg, J., Basler, C.A., Jacobs, J.R., Kennedy, E.D., Tomasi, S., Trout, D., Hornsby-Myers, J., Oussayef, N.L., Delaney, L.J., Patel, K., Shetty, V., Kline, K.E., Schroeder, B., Herlihy, R.K., House, J., Jervis, R., Clayton, J.L., Ortbahn, D., Austin, C., Berl, E., Moore, Z., Buss, B.F., Stover, D., Westergaard, R., Pray, I., DeBolt, M., Person, A., Gabel, J., Kittle, T.S., Hendren, P., Rhea, C., Holsinger, C., Dunn, J., Turabelidze, G., Ahmed, F.S., deFijter, S., Pedati, C.S., Rattay, K., Smith, E.E., Luna-Pinto, C., Cooley, L.A., Saydah, S., Preacely, N.D., Maddox, R.A., Lundeen, E., Goodwin, B., Karpathy, S.E., Griffing, S., Jenkins, M.M., Lowry, G., Schwarz, R.D., Yoder, J., Peacock, G., Walke, H.T., Rose, D.A., Honein, M.A., 2020. COVID-19 Among Workers in Meat and Poultry Processing Facilities - 19 States, April 2020. MMWR Morb Mortal Wkly Rep 69.

Fontanet, A., Tondeur, L., Grant, R., Temmam, S., Madec, Y., Bigot, T., Grzelak, L., Cailleau, I., Besombes, C., Ungeheuer, M.-N., Renaudat, C., Perlaza, B.L., Arowas, L., Jolly, N., Pellerin, S.F., Kuhmel, L.,

Staropoli, I., Huon, C., Chen, K.-Y., Crescenzo-Chaigne, B., Munier, S., Charneau, P., Demeret, C., Bruel, T., Eloit, M., Schwartz, O., Hoen, B., 2021. SARS-CoV-2 infection in schools in a northern French city: a retrospective serological cohort study in an area of high transmission, France, January to April 2020. Eurosurveillance 26.
Günther, T., Czech-Sioli, M., Indenbirken, D., Robitaille, A., Tenhaken, P., Exner, M., Ottinger, M., Fischer, N., Grundhoff, A., Brinkmann, M.M., 2020. SARS-CoV-2 outbreak investigation in a German meat processing plant. EMBO Mol Med 12, e13296.
Han, J., Zhang, X., He, S., Jia, P., 2020. Can the coronavirus disease be transmitted from food? A review of evidence, risks, policies and knowledge gaps. Environ Chem Lett, 1-12.
He, J., Guo, Y., Mao, R., Zhang, J., 2021. Proportion of asymptomatic coronavirus disease 2019: A systematic review and meta-analysis. J Med Virol 93, 820-830.
Hobbs, J.E., 2021. The Covid-19 pandemic and meat supply chains. Meat Sci, 108459.
Jones, T.C., Biele, G., Muhlemann, B., Veith, T., Schneider, J., Beheim-Schwarzbach, J., Bleicker, T., Tesch, J., Schmidt, M.L., Sander, L.E., Kurth, F., Menzel, P., Schwarzer, R., Zuchowski, M., Hofmann, J., Krumbholz, A., Stein, A., Edelmann, A., Corman, V.M., Drosten, C., 2021. Estimating infectiousness throughout SARS-CoV-2 infection course. Science 373.
Kennedy, M., Lee, S.J., Epstein, M., 2021. Modeling aerosol transmission of SARS-CoV-2 in multi-room facility. J Loss Prev Process Ind 69, 104336.
Lau, E.H.Y., Leung, G.M., 2020. Reply to: Is presymptomatic spread a major contributor to COVID-19 transmission? Nat Med 26, 1534-1535.
Leech, G., Rogers-Smith, C., Monrad, J.T., Sandbrink, J.B., Snodin, B., Zinkov, R., Rader, B., Brownstein, J.S., Gal, Y., Bhatt, S., Sharma, M., Mindermann, S., Brauner, J.M., Aitchison, L., 2022. Mask wearing in community settings reduces SARS-CoV-2 transmission. Proceedings of the National Academy of Sciences 119.
Li, F., Wang, J., Liu, Z., Li, N., 2022. Surveillance of SARS-CoV-2 Contamination in Frozen Food-Related Samples - China, July 2020 - July 2021. China CDC Wkly 4, 465-470.
Ma, Q., Liu, J., Liu, Q., Kang, L., Liu, R., Jing, W., Wu, Y., Liu, M., 2021. Global Percentage of Asymptomatic SARS-CoV-2 Infections Among the Tested Population and Individuals With Confirmed COVID-19 Diagnosis: A Systematic Review and Meta-analysis. JAMA Netw Open 4, e2137257.
Magnusson, K., Nygård, K., Methi, F., Vold, L., Telle, K., 2021. Occupational risk of COVID-19 in the first versus second epidemic wave in Norway, 2020. Euro Surveill 26.
Mallet, Y., Pivette, M., Revest, M., Angot, E., Valence, M., Dupin, C., Picard, N., Brelivet, G., Seyler, T., Ballet, S., Le Tertre, A., Guillois, Y., 2021. Identification of Workers at Increased Risk of Infection During a COVID-19 Outbreak in a Meat Processing Plant, France, May 2020. Food Environ Virol, 1-9.
Migale, I., 2020. Migale bioinformatics Facility.
Miller, S.L., Nazaroffw, W.W., Jimenez, J.L., Boerstra, A., Buonannos, G., Dancer, S.J., Kurnitski, J., Marrs, L.C., Morawska, L., Noakes, C., 2020. Transmission of SARS-CoV-2 by inhalation of respiratory aerosol in the Skagit Valley Chorale superspreading event. Indoor Air.
Ming, Z., Han, S., Deng, K., Reyes, E., Ha, Y., Kim, S., Zhao, Y., Dobritsa, A., Wu, M., Zhang, D., Cox, D.P., Joyner, E., Kulasekara, H., Kim, S.H., Jang, Y.S., Fowler, C., Fei, X., Akasaki, H., Themeli, E., Agapov, A., Bruneau, D., Tran, T., Szczesny, C., Kienzle, C., Tenney, K., Geng, H., Myoda, S., Samadpour, M., 2021. Prevalence of SARS-CoV-2 contamination on food plant surfaces as determined by environmental monitoring. J Food Prot.
Parker, C.W., Singh, N., Tighe, S., Blachowicz, A., Wood, J.M., Seuylemezian, A., Vaishampayan, P., Urbaniak, C., Hendrickson, R., Laaguiby, P., Clark, K., Clement, B.G., O'Hara, N.B., Couto-Rodriguez, M., Bezdan, D., Mason, C.E., Venkateswaran, K., 2020. End-to-End Protocol for the Detection of SARS-CoV-2 from Built Environments. mSystems 5.
Pitol, A.K., Julian, T.R., 2021. Community Transmission of SARS-CoV-2 by Surfaces: Risks and Risk Reduction Strategies. Environmental Science & Technology Letters 8, 263-269.
Pokora, R., Kutschbach, S., Weigl, M., Braun, D., Epple, A., Lorenz, E., Grund, S., Hecht, J., Hollich, H., Rietschel, P., Schneider, F., Sohmen, R., Taylor, K., Dienstbuehl, I., 2021. Investigation of

superspreading COVID-19 outbreak events in meat and poultry processing plants in Germany: A cross-sectional study. PLoS ONE 16, e0242456.
R Core Team, D.T., 2022. R: A language and environment for statistical computing. R Foundation for Statistical Computing, Vienna, Austria.
Sah, P., Fitzpatrick, M.C., Zimmer, C.F., Abdollahi, E., Juden-Kelly, L., Moghadas, S.M., Singer, B.H., Galvani, A.P., 2021. Asymptomatic SARS-CoV-2 infection: A systematic review and meta-analysis. Proc Natl Acad Sci U S A 118.
Santé Publique France, S., 2020. Covid-19: point épidémiologique du 20 août 2020.
Steinberg, J., Kennedy, E.D., Basler, C., Grant, M.P., Jacobs, J.R., Ortbahn, D., Osburn, J., Saydah, S., Tomasi, S., Clayton, J.L., 2020. COVID-19 Outbreak Among Employees at a Meat Processing Facility - South Dakota, March-April 2020. MMWR Morb Mortal Wkly Rep 69, 1015-1019.
Teyssou, E., Delagreverie, H., Visseaux, B., Lambert-Niclot, S., Brichler, S., Ferre, V., Marot, S., Jary, A., Todesco, E., Schnuriger, A., Ghidaoui, E., Abdi, B., Akhavan, S., Houhou-Fidouh, N., Charpentier, C., Morand-Joubert, L., Boutolleau, D., Descamps, D., Calvez, V., Marcelin, A.G., Soulie, C., 2021. The Delta SARS-CoV-2 variant has a higher viral load than the Beta and the historical variants in nasopharyngeal samples from newly diagnosed COVID-19 patients. J Infect 83, e1-e3.
van Kampen, J.J.A., van de Vijver, D., Fraaij, P.L.A., Haagmans, B.L., Lamers, M.M., Okba, N., van den Akker, J.P.C., Endeman, H., Gommers, D., Cornelissen, J.J., Hoek, R.A.S., van der Eerden, M.M., Hesselink, D.A., Metselaar, H.J., Verbon, A., de Steenwinkel, J.E.M., Aron, G.I., van Gorp, E.C.M., van Boheemen, S., Voermans, J.C., Boucher, C.A.B., Molenkamp, R., Koopmans, M.P.G., Geurtsvankessel, C., van der Eijk, A.A., 2021. Duration and key determinants of infectious virus shedding in hospitalized patients with coronavirus disease-2019 (COVID-19). Nat Commun 12, 267.
Watanabe, T., Bartrand, T.A., Weir, M.H., Omura, T., Haas, C.N., 2010. Development of a dose-response model for SARS coronavirus. Risk Anal 30, 1129-1138.
Weersink, A., von Massow, M., Bannon, N., Ifft, J., Maples, J., McEwen, K., McKendree, M., Nicholson, C., Novakovic, A., Rangarajan, A., Richards, T., Rickard, B., Rude, J., Schipanski, M., Schnitkey, G., Schulz, L., Schuurman, D., Schwartzkopf-Genswein, K., Stephenson, M., Thompson, J., Wood, K., 2020. COVID-19 and the agri-food system in the United States and Canada. Agric Syst, 103039.
Zhao, S., Tang, B., Musa, S.S., Ma, S., Zhang, L., Zeng, M., Yun, Q., Guo, W., Zheng, Y., Yang, Z., Peng, Z., Chong, M.K., Javanbakht, M., He, D., Wang, M.H., 2021. Estimating the generation interval and inferring the latent period of COVID-19 from the contact tracing data. Epidemics 36, 100482.

Highlight

- Mask-wearing reduces the contamination of surfaces and meat cuts by SARS-CoV-2
- Production losses can be important if no COVID-19 preventive measures are taken
- Mask-wearing has strong influence on COVID-19 cluster occurrence in food facilities